Scene Matching on Imagery

- There are a plethora of algorithms in existence for automatic scene matching, each with particular strengths and weaknesses
- SAR scenic matching for interferometry applications is difficult for several reasons:
  - Thermal noise causes the fine structure of two SAR images to differ, adding noise to the correlation measurements.
  - Geometric speckle noise is similar in images acquired in nearly the same geometry, but as the interferometric baseline increases, differing speckle noise corrupts the matching correlation.
  - Scene decorrelation is another form of speckle noise difference that corrupts matching correlation.
- SAR scenic matching for mosaicking applications involves greater challenges, including severe speckle noise differences, layover and shadow effects.

Automatic Scene Matching

- Find overlap region and sample points at specified spacing in along track and cross track direction.
- Typical window sizes are 64x64 pixels for image data and 64x64 or 128x128 pixels for height data.
- Uses a modified Frankot's method for rejecting bad matches and to provide an estimate of the match covariance matrix.
- Cross correlation uses a normalized mean correlation function, mean of search window is calculated over the region in common with the reference window.

Mean of reference is constant

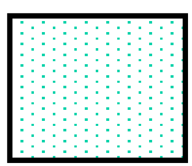

Reference Window

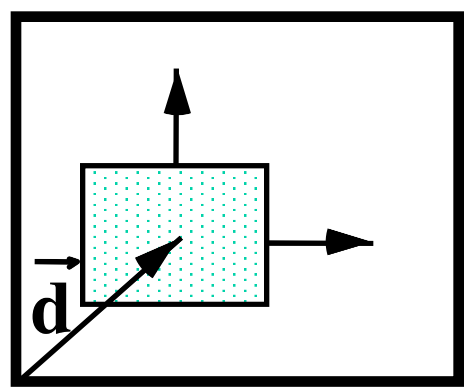

Search Window

Mean of search varies with position

Match Correlation Estimate

- Correlation is computed in the spatial domain using a normalized cross correlation algorithm.
- Let $I_1(\vec{x})$ be the image values at a point $\vec{x}$ in the reference window in the first data set, $\bar{I}_1$, the mean of the intensities in that window.
- Let $I_2(\vec{x}+\vec{d})$ be the image value at point $\vec{x}+\vec{d}$ in the search window of the second data set, and $\bar{I}_2(\vec{d})$ the mean of the intensities in that window.
- Viewing each image as a vector in an n-dimensional vector space then the cross correlation is computed as

$$c(\vec{d}) = \frac{\left\langle I_1 - \bar{I}_1, I_2(\vec{d}) - \bar{I}_2(\vec{d}) \right\rangle}{\sqrt{\left|I_1 - \bar{I}_1\right| \left|I_2(\vec{d}) - \bar{I}_2(\vec{d})\right|}} = \frac{\left\langle I_1 - \bar{I}_1, I_2(\vec{d}) - \bar{I}_2(\vec{d}) \right\rangle}{\sigma_{I_1}\sigma_{I_2(\vec{d})}}$$

where σ_{I_1} **and** $\sigma_{I_2(\vec{d})}$ **are the standard deviations of the image intensities in data sets 1 and 2, respectively.**

Space-domain correlation used for speed and because large irregular data gaps are trouble free.

Baseline Estimation from Offsets

- Baseline estimation in repeat pass interferometry is a rich subject, and will be covered completely in a separate module. Briefly:
- Offset field determined from scene matching carries information sufficient to reconstruct the baseline to an accuracy com-mensurate with ability to co-register images.
- For nearly parallel, smoothly varying, orbit tracks, the baseline can be modeled as a simple function of the range ρ

$$B_{\parallel}(\rho) \approx B\sin(\theta_0(\rho) - \alpha) = \Delta\rho(\rho)$$

$$B_{\perp}(\rho) \approx B\cos(\theta_0(\rho) - \alpha) = \frac{d\Delta\rho}{d\theta}(\rho)$$

- **Solve two equations for two unknowns:** B, α
- **Evaluating baseline at several widely-spaced along-track (azimuth) locations gives azimuth history of the baseline.**

Converging Baselines

- For orbit tracks with substantial convergence, azimuth offsets strongly characterize convergence rates.

Observation vector:

$$\{\cdots, \Delta\rho(\rho_i, a_i), \Delta a(\rho_i, a_i), \Delta\rho(\rho_{i+1}, a_{i+1}), \Delta a(\rho_{i+1}, a_{i+1}), \cdots\}$$

Parameter vector: $\{B_{s0}, B_{c0}, B_{h0}, \gamma, \frac{\partial B_c}{\partial s}, \frac{\partial B_h}{\partial s}\}$

where γ is an image scaling factor resulting from velocity differences between the tracks, and (*s,c,h*) are local coordinates defined by the orbit track (see notes on coordinate systems).

Slant range plane seen from above

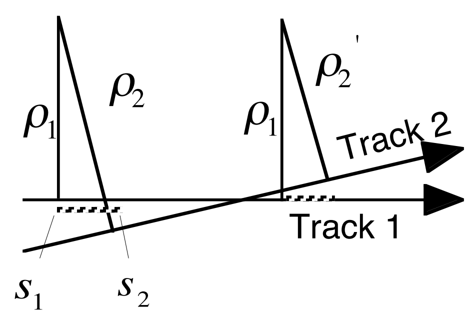

Baseline Accuracy from Offsets

- Baselines determined from offset fields are typically accurate to a fraction of the scene matching accuracy that depends on the model function and the number of offset estimates. Example:
  - Zero baseline image pair with 10 match points across range.
  - Scene matching accuracy of 1/20 pixel resolution at typical single look resolution of 15 meters: 75 cm / 3 = 25 cm
- This accuracy is insufficient for topographic mapping applications

$$\sigma_h = \frac{\rho}{B} \sin\theta \cos\alpha \sigma_{B_z}$$

$$= 320 \text{ m} \quad ; \quad \rho = 830 \text{ km}, \; B = 250 \text{ m}, \theta = 23^{\circ}, \alpha = 0, \sigma_{B_z} = 25 \text{ cm}$$

These geometric parameters are typical of ERS with baselines suitable for topography. Generally, ground control points tied to the unwrapped interferometric phase are required for mapping.

Interferogram Formation

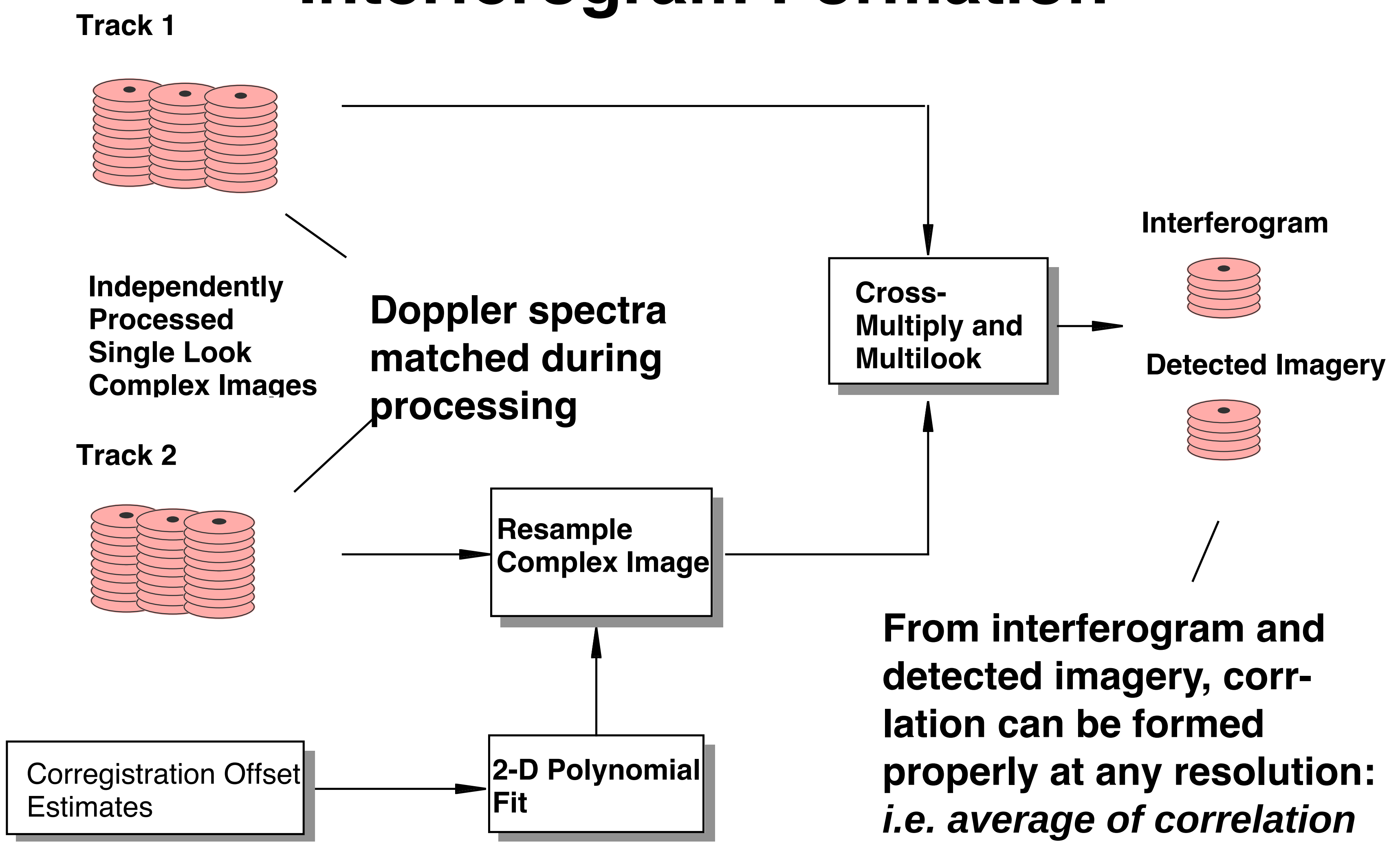

From interferogram and detected imagery, corr-lation can be formed properly at any resolution:
i.e. average of correlation is not correlation of average

Registration Implementation

- In resampling single look complex image to register properly with the reference image, care must be taken in interpolation of complex data
  - The azimuth spectrum of squinted SAR data is centered at the Doppler centroid frequency - a band-pass signal
  - Simple interpolators, such as linear or quadratic interpolators, are low-pass filters and can destroy band-pass data characteristics
- Band-pass interpolators or spectral methods preserve phase fidelity

SIGNAL SPECTRUM (1-D)

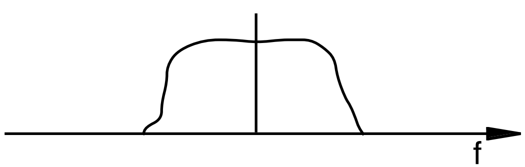

LOW PASS SIGNAL

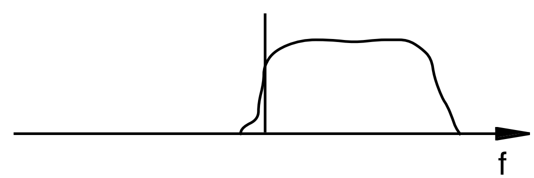

BAND PASS SIGNAL

Repeat Pass Interferometry Back-end Processing

<u>Performance Summary:</u>
L-band: good over most terrain
C-band: poor over most terrain

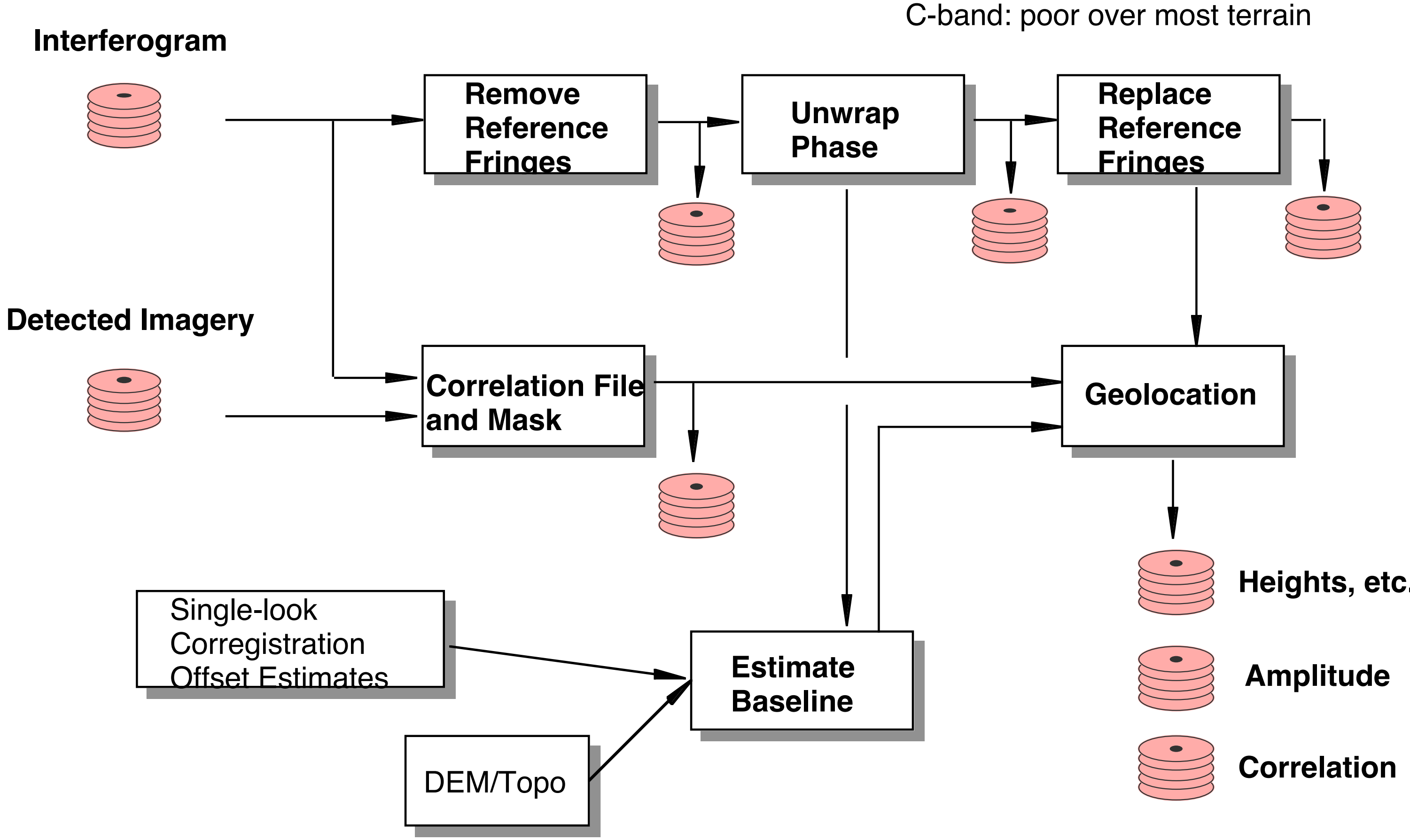

N-pass Differential Processing